Electronic Supplementary Material (ESI) for Journal of Materials Chemistry C.

Electronic Supplementary Information for:

Yttria-stabilized zirconia microspheres: Novel building blocks for high-temperature photonics

Elisabeth W. Leib[1], Robert M. Pasquarelli[2], Jefferson J. do Rosário[2], Pavel N. Dyachenko[3], Sebastian Döring[1], Anke Puchert[1], Alexander Yu. Petrov[3,4], Manfred Eich[3], Gerold A. Schneider[2], Rolf Janssen[2], Horst Weller[1,5,6] and Tobias Vossmeyer[1]*

[1] Institute of Physical Chemistry, University of Hamburg, Grindelallee 117, D-20146 Hamburg, Germany.

[2] Institute of Advanced Ceramics, Hamburg University of Technology (TUHH), Denickestraße 15, 21073 Hamburg, Germany.

[3] Institute for Optical and Electronic Materials, Hamburg University of Technology (TUHH), Eissendorfer Straße 38, 21073 Hamburg, Germany

[4] ITMO University, 49 Kronverskii Ave., 197101, St. Petersburg, Russia

[5] The Hamburg Centre for Ultrafast Imaging, Luruper Chaussee 149, 22761 Hamburg, Germany.

[6] Department of Chemistry, Faculty of Science, King Abdulaziz University, Jeddah, Saudi Arabia.

*tobias.vossmeyer@chemie.uni-hamburg.de

1. Particle synthesis

1.1. Synthetic details

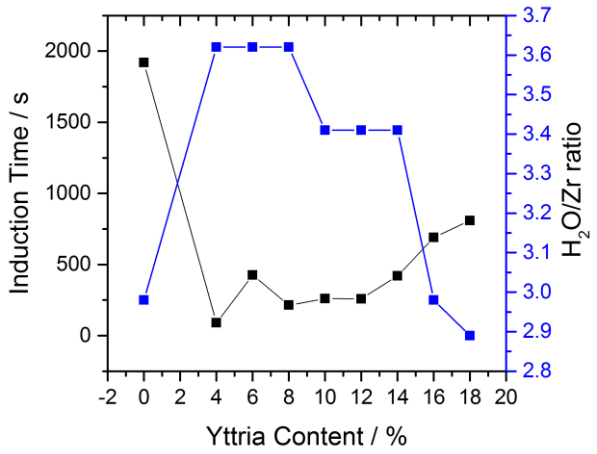

Figure S 1. Induction times and zirconia precursor-to-water molar ratios as a function of the target yttria content.

Table S 1. Amount of added yttrium *iso*-propoxide precursor, resulting target yttrium content (Y/(Y+Zr)), added amount of water and resulting water-to-zirconium *n*-propoxide molar ratio.

Sample	Yttrium isopropoxide / mg	Y/(Y+Zr)	Water / mL	Water / zirconium *n*-propoxide ratio
Y4*	136	3.77%	0.850	3.62
Y6*	210	5.70%	0.850	3.62
Y8	601	8.00%	1.700	3.62
Y10	770	10.00%	1.600	3.41
Y12	954	12.10%	1.600	3.41
Y14	1150	14.20%	1.600	3.41
Y16*	669	16.16%	0.700	2.98
Y18*	749	17.75%	0.675	2.89

* For these samples only a half batch-size was synthesized. The reasons were for samples Y4 and Y6 the sufficiently high yield with a half batch and for samples Y16 and Y18 the high amount of costly yttrium *iso*-propoxide necessary.

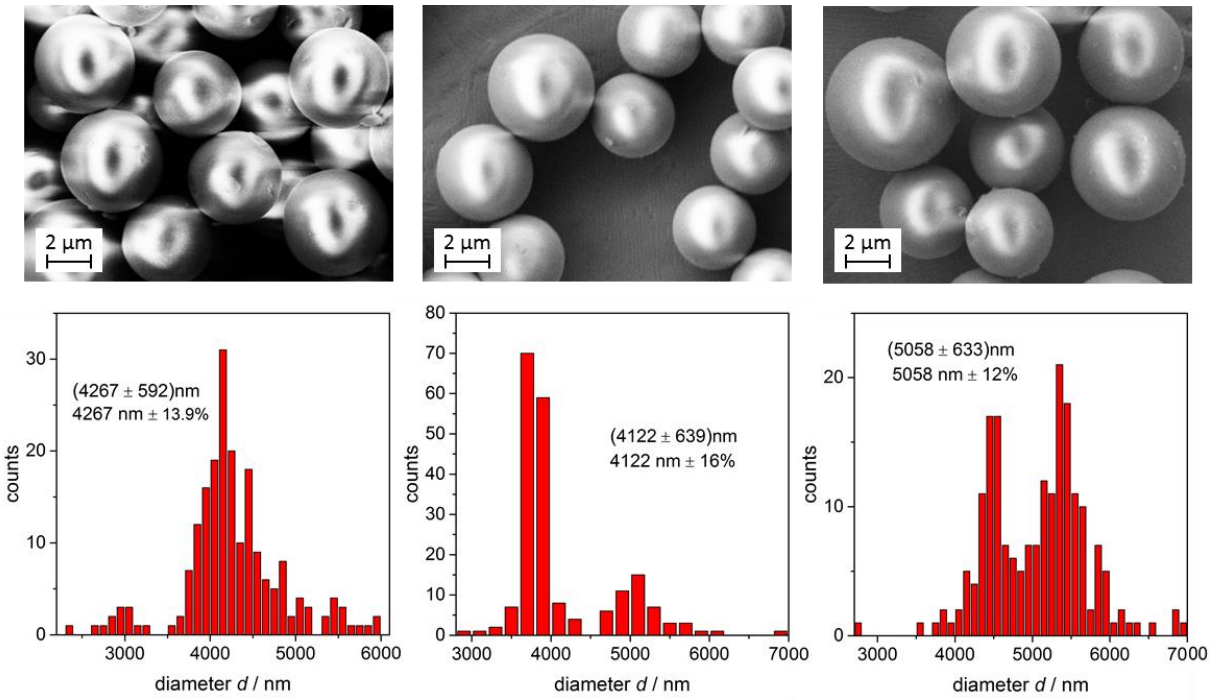

Figure S 2. Larger particle samples YPG0, YPG6 and YPG10 with SEM micrographs (top row) and size distributions (bottom row).

Table S 2. Synthetic parameters for the fabrication of the larger particle samples YPG0, YPG6 and YPG10 including amounts of starting material, extended stirring times, reaction temperatures and ageing conditions.

	YPG0	YPG6	YPG10
eicosanoic acid	1.31 g	1.31 g	1.31 g
water	1.400 mL	1.600 mL	1.500 mL
extended stirring	5 min 30 s	4 min	4 min 35 s
temperature during reaction	42 °C	50 °C	50 °C
temperature during ageing	RT	RT	~70 °C
tube roller rotation speed	5 rpm	9 rpm	5 rpm
ageing time	150 min	90 min	120 min

1.2. Sample overview

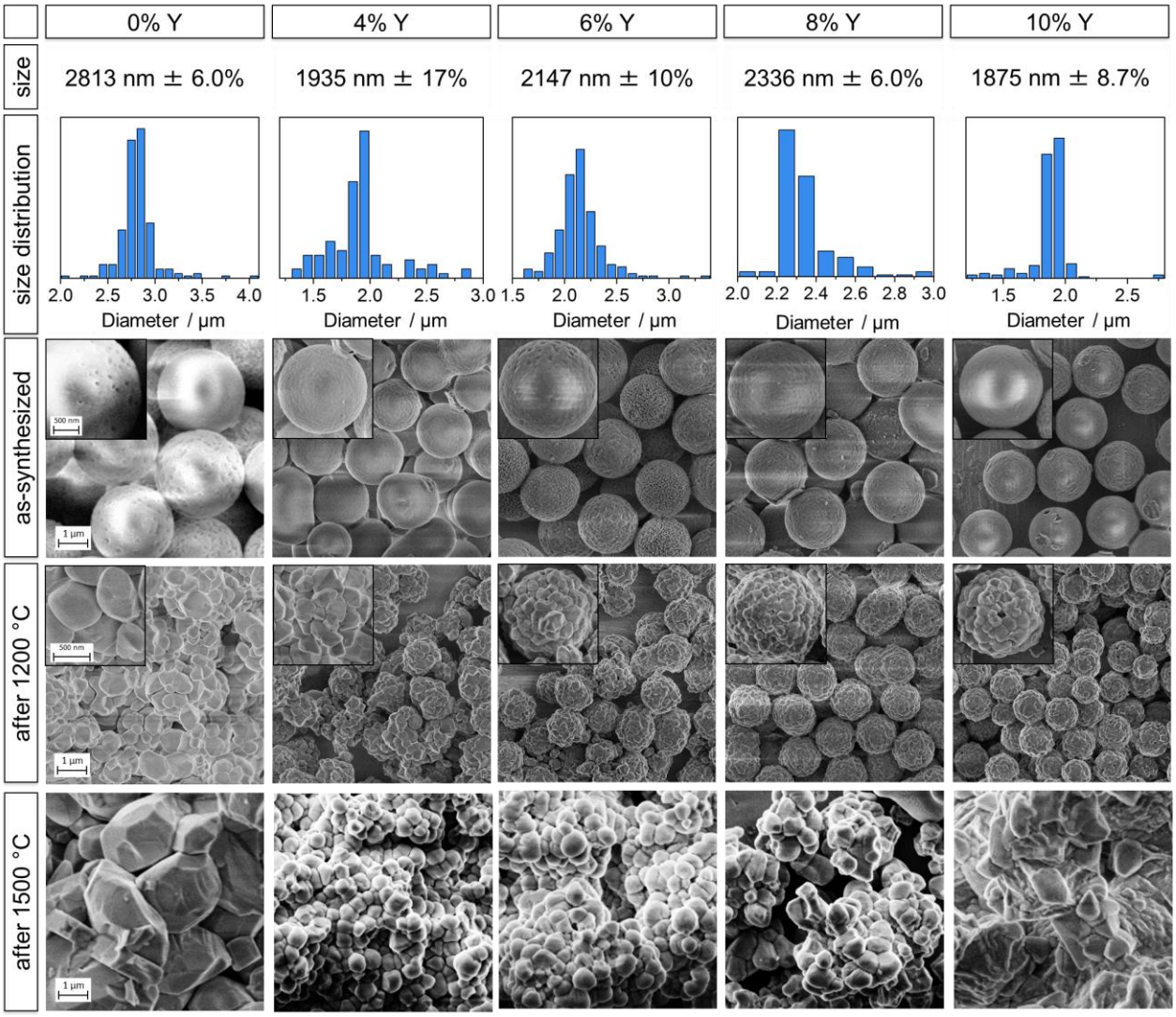

Figure S 3. Undoped zirconia microparticle sample (0% Y) and yttria-stabilized zirconia particles with added yttrium amounts of 4, 6, 8, and 10% (from left to right). Diameter sizes with standard deviations (first row), size distributions (second row), SEM images of as-synthesized particles (third row), of particles heated at 1200 °C for 3 h (fourth row) and particles heated at 1500 °C for 3 h (fifth row). Scale bars apply to all images and insets within a given row.

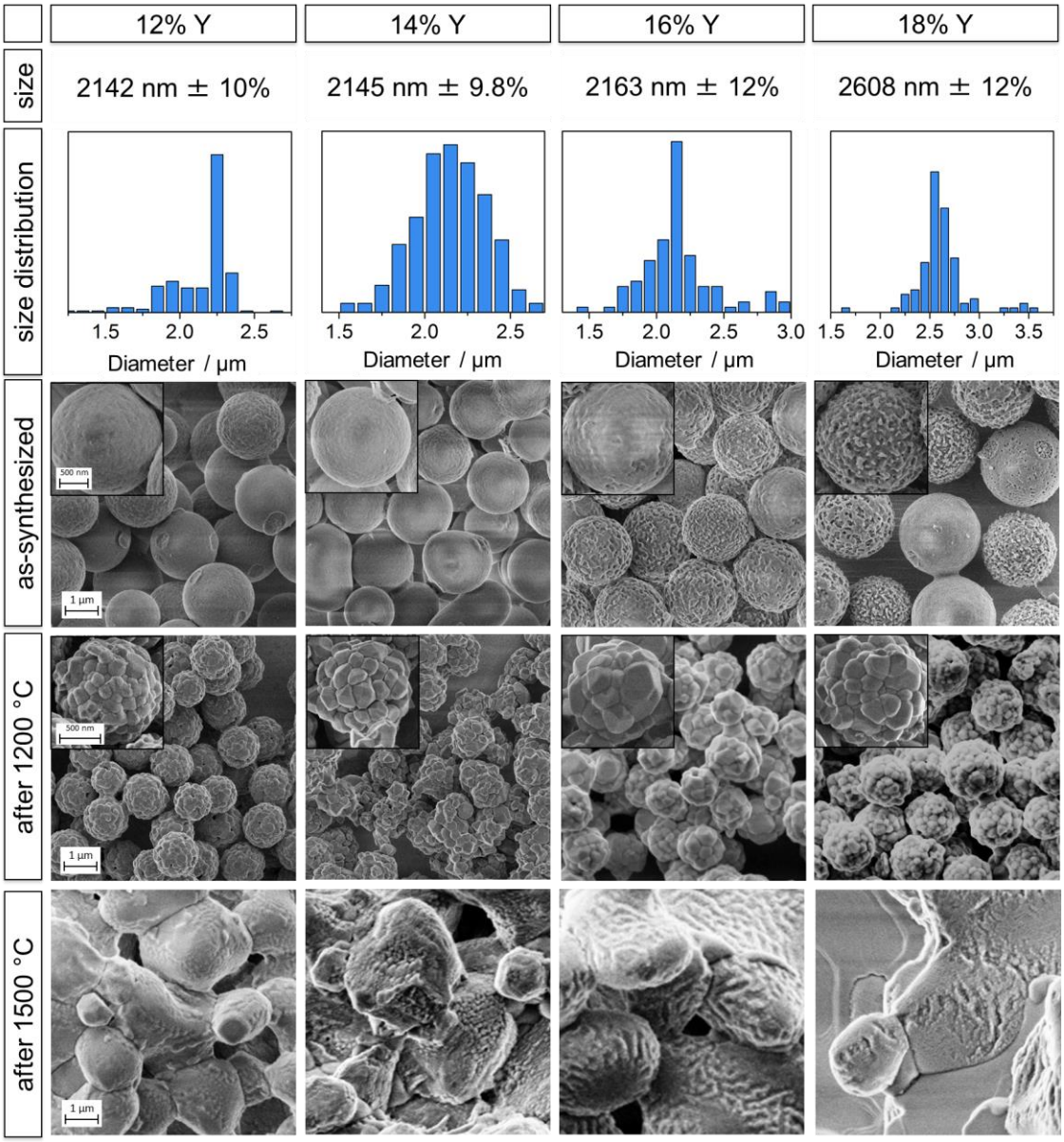

Figure S 4. Yttria-stabilized zirconia particles with added yttrium amounts of 12, 14, 16 and 18% (from left to right). Diameter sizes with standard deviations (first row), size distributions (second row), SEM images of as-synthesized particles (third row), of particles heated at 1200 °C for 3 h (fourth row) and particles heated at 1500 °C for 3 h (fifth row). Scale bars apply to all images and insets within a given row.

2. Heat treatment

2.1. Heating of the particles

The as-synthesized particles were dried at 80 °C under air for 4 h. The obtained powder samples were heated step-wise in a muffle oven (L9/SKM, Nabertherm) at 250, 450, 650 and 850 °C for 1 h each. High temperature anneals were performed in a tube furnace (STF 16/100, Carbolite) by heating step-wise with 3 h holds at 120, 450, 850, 1200 and 1500 °C. For all heat treatments, heating and cooling rates of 5 °C/min were used. The heating rate profiles are shown in Figure S 5.

The crystal structure of the samples after heating was investigated by powder X-ray diffraction (XRD) using a Philips X'Pert PRO MPD with Cu-K_α radiation and a Bragg-Brentano geometry. Grain sizes were calculated using the Scherrer equation with the full width at half maximum (FWHM) obtained from Lorentz fits of the peaks in the X-ray diffractograms, using the (101) and (11-1) reflexes for the tetragonal and monoclinic structure, respectively. The instrumental broadening of 0.06° was taken into account, enabling estimations of the maximum grain size up to ~80 nm. For samples heated to 1200 and 1500 °C the diffraction patterns were subjected to a $K_{\alpha 2}$ correction with the software X'Pert HighScore Plus. The particle morphology and stability were assessed by scanning electron microscopy (SEM, EVO MA 10 and a Leo Type 1550 Gemini, both Zeiss). The particle sizes and size standard deviations were measured using SEM micrographs by counting between 100 and 200 particles per batch with the software ImageJ. Grain sizes of the particles after heating to 1200 and 1500 °C were determined using the linear intercept method from SEM micrographs by counting 100 and 50 grains per sample, respectively. It was made sure to avoid the particle edges so as to eliminate distortions resulting from curvature of the particles. Exemplary SEM micrographs are shown in Figure S 6.

The particle composition was analyzed by inductively coupled plasma optical emission spectroscopy (ICP-OES, Spectro Model ARCOS spectrometer) and energy-dispersive X-ray spectroscopy (EDX, INCAx-act from Oxford instruments with a 10 mm^2 silicon drift detector). ICP-OES samples were prepared by salt fusion in a 50 wt% mixture of sodium/potassium carbonate and lithium metaborate followed by dissolution in 8% nitric acid-deionized water.

Particle stability to resuspension was assessed by suspending 5–10 mg per particle sample in 5–10 drops of ethanol with the help of a sonicator (Badelin, Sonorex Super RK 106) for at least 5 min.

Photonic glass films were heated in a tube furnace with a 5 °C/min heating rate and a 10 °C/min cooling rate, each sequentially at 700, 1000, 1200, 1300, and 1400 °C for 3 h at each temperature. Films were

then heated longer at 1400 °C for a total of 24, 72, and 192 h. XRD, SEM, and optical reflectance measurements were performed after each heat treatment. A Fourier transform infrared (FTIR) spectrometer (Vertex 70, Bruker) equipped with a gold-coated integrating sphere accessory and an MCT detector was used to measure the hemispherical diffuse reflectance of the films in the infrared region between 1–6 µm.

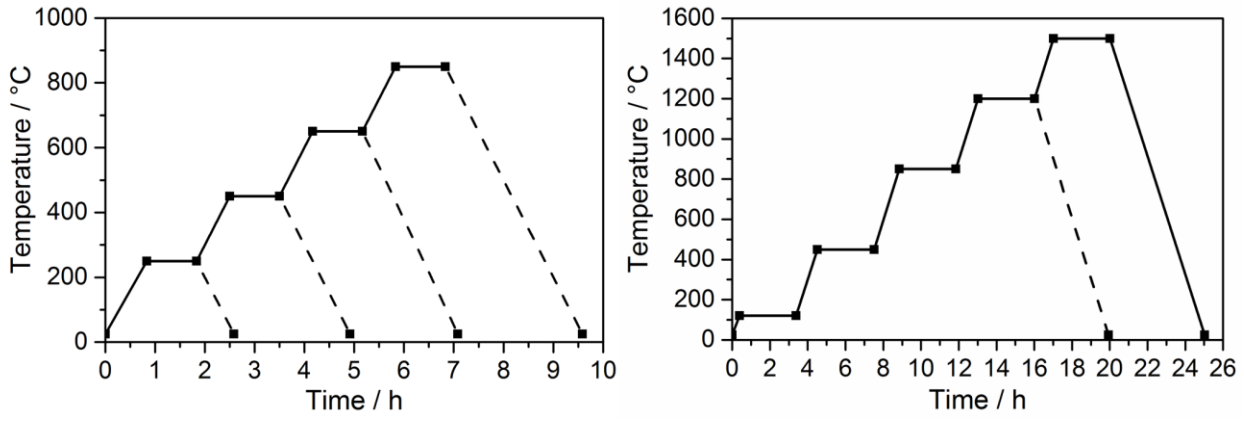

Figure S 5. Heating profiles used for the heating experiments in the muffle oven up to 850 °C (left) and in the tube furnace for 1200 and 1500 °C (right). All heating and cooling rates were 5 °C/min.

2.2. Grain size analysis

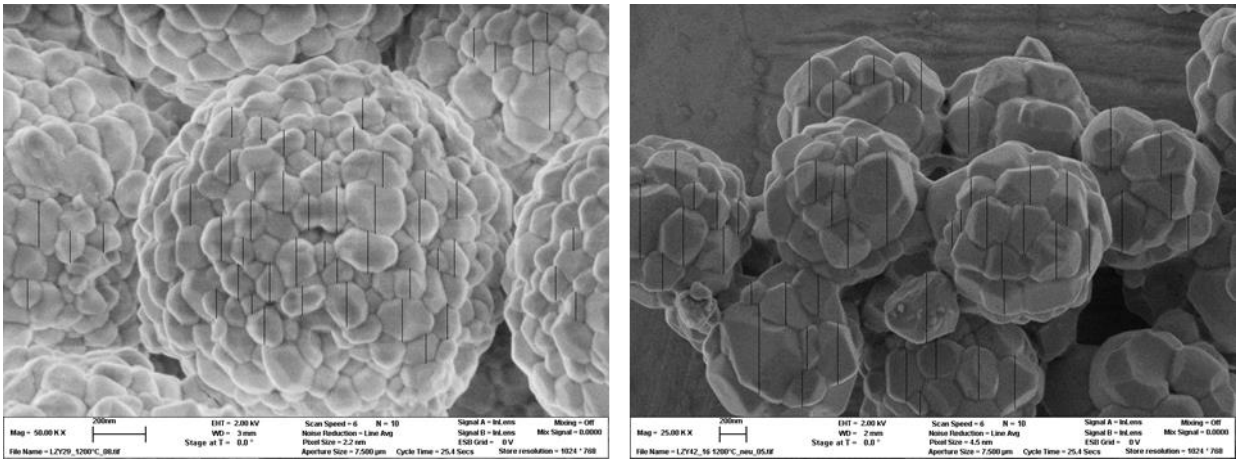

Figure S 6. Exemplary SEM micrographs used for the grain size determination. Samples displayed are Y8 (left) and Y16 (right) after heating at 1200 °C for 3 h.

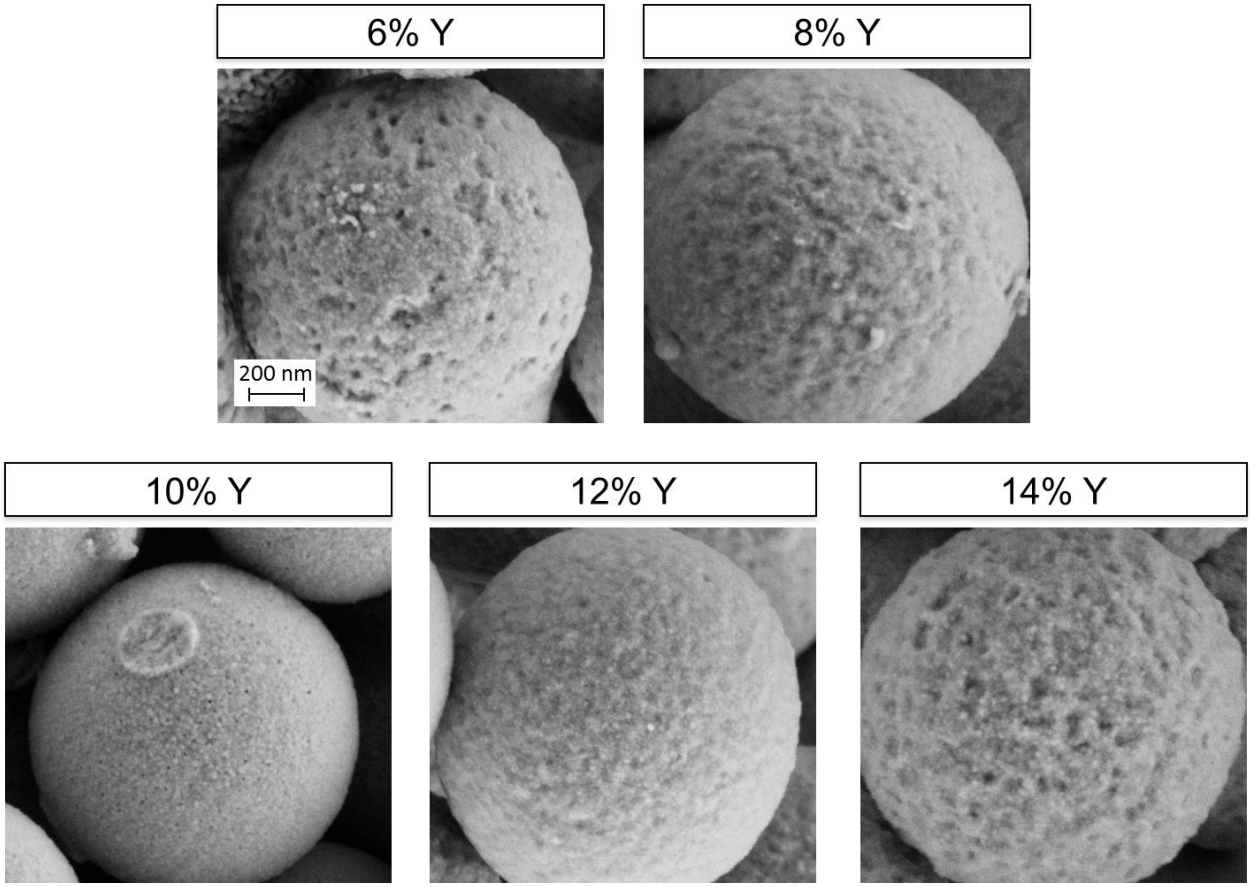

Figure S 7. SEM micrographs of YSZ particle samples Y6, Y8, Y10, Y12 and Y14 after heating at 850 °C. Small grains with sizes ≤25 nm are discernible.

3. X-ray diffraction

3.1. Particle X-ray diffractograms

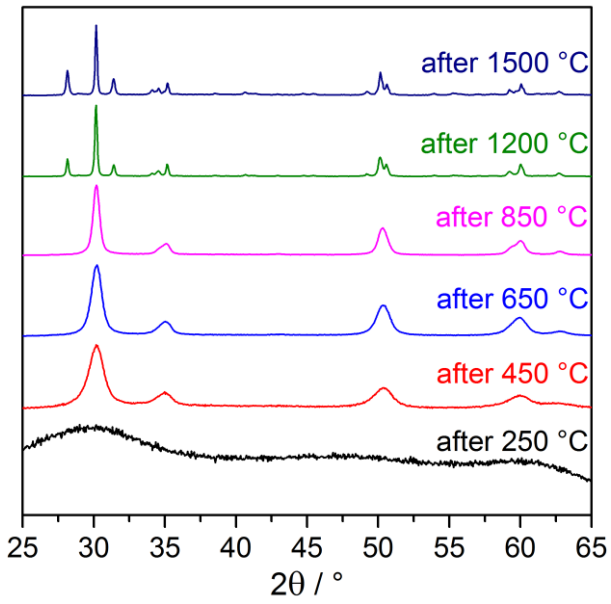

Figure S 8. X-ray diffractograms for sample Y6 heated to 250, 450, 650, 850, 1200 and 1500 °C (bottom to top). After heating to 450 °C the sample had transitioned to the tetragonal phase and after heating to ≥1200 °C a fraction of the sample transitioned to the monoclinic phase.

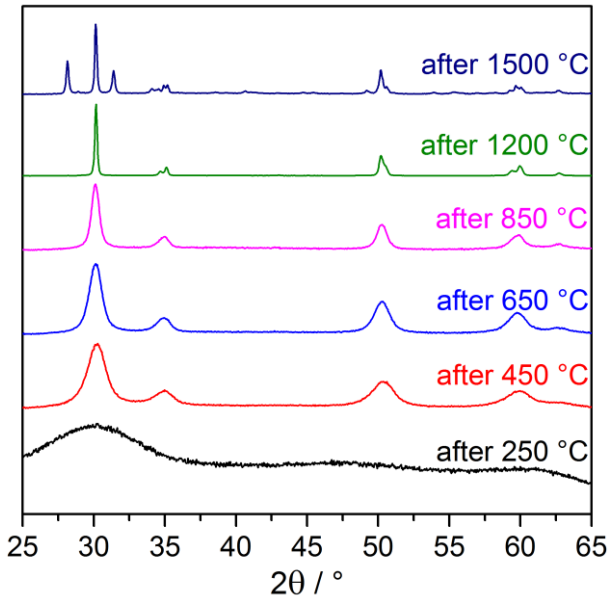

Figure S 9. X-ray diffractograms for sample Y8 heated to 250, 450, 650, 850, 1200 and 1500 °C (bottom to top). After heating to 450 °C the sample had transitioned to the tetragonal phase and after heating to 1500 °C a fraction of the sample transitioned to the monoclinic phase.

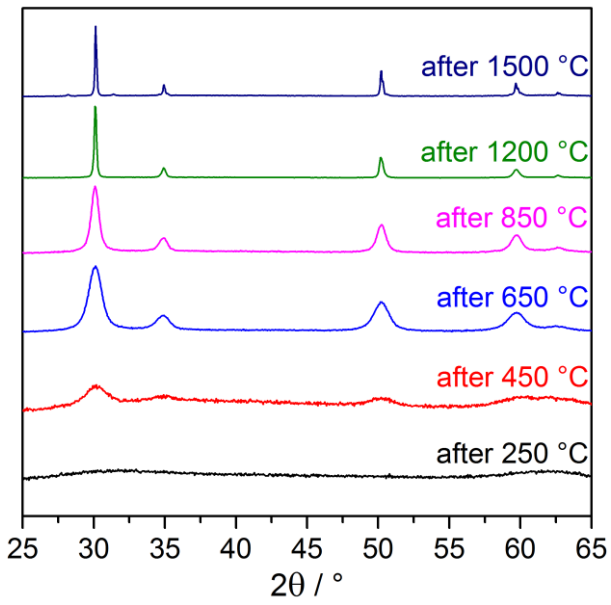

Figure S 10. X-ray diffractograms for sample Y10 heated to 250, 450, 650, 850, 1200 and 1500 °C (bottom to top). After heating to 450 °C the sample had transitioned to the cubic phase. After heating to 1500 °C very faint monoclinic peaks were visible.

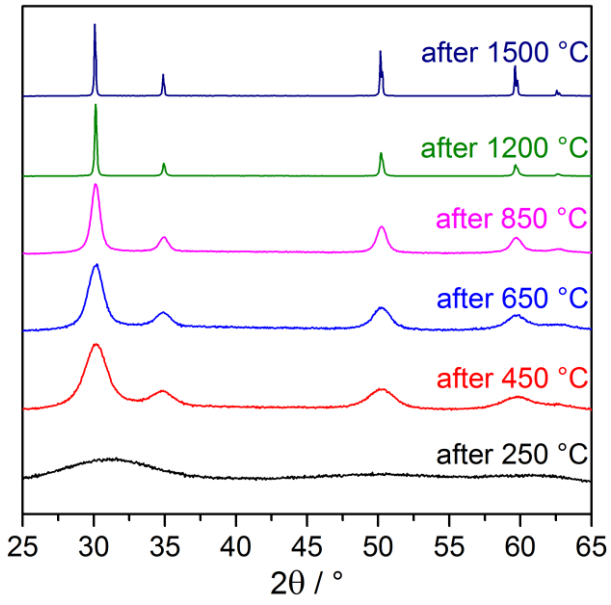

Figure S 11. X-ray diffractograms for sample Y12 heated to 250, 450, 650, 850, 1200 and 1500 °C (bottom to top). After heating to 450 °C the sample had transitioned to the cubic phase and remained that way even after heating to 1500 °C.

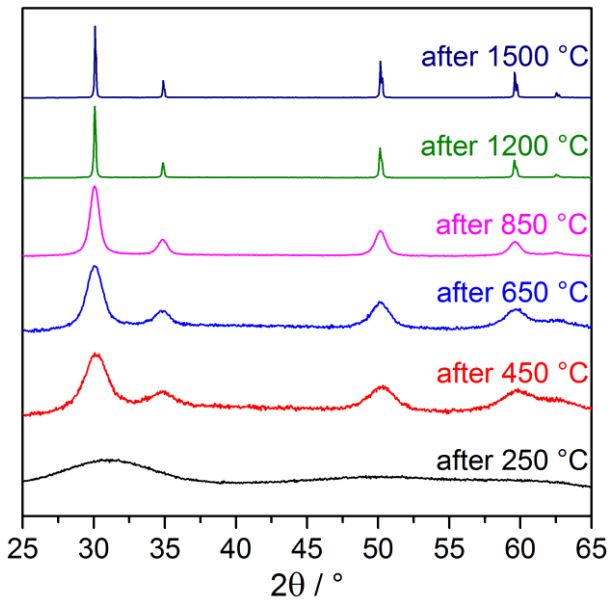

Figure S 12. X-ray diffractograms for sample Y14 heated to 250, 450, 650, 850, 1200 and 1500 °C (bottom to top). After heating to 450 °C the sample had transitioned to the cubic phase and remained that way even after heating to 1500 °C.

4. Photonic glasses

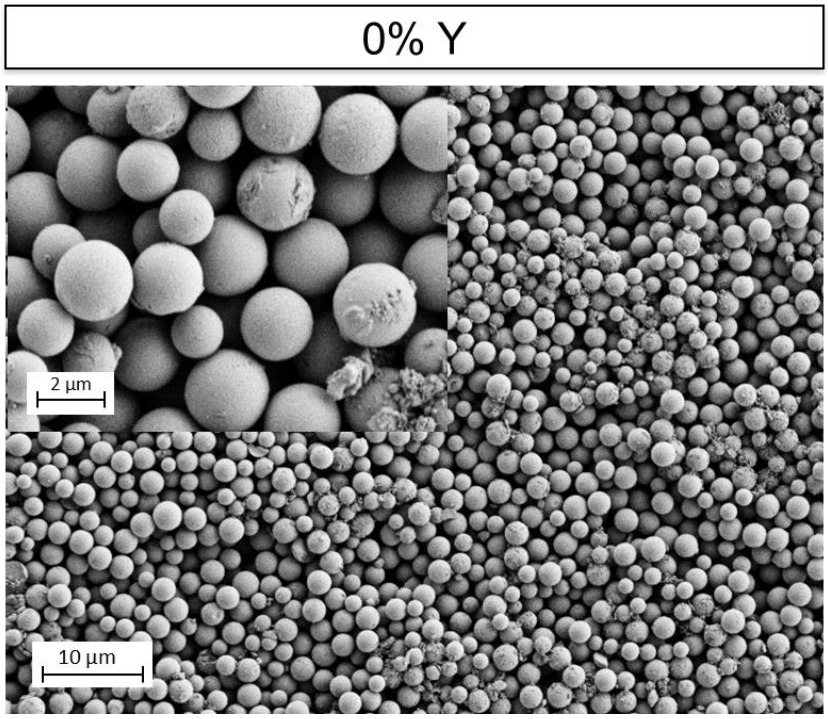

Figure S 13. Film F0 assembled from particle sample YPG0 after heating at 700 °C for 3h.

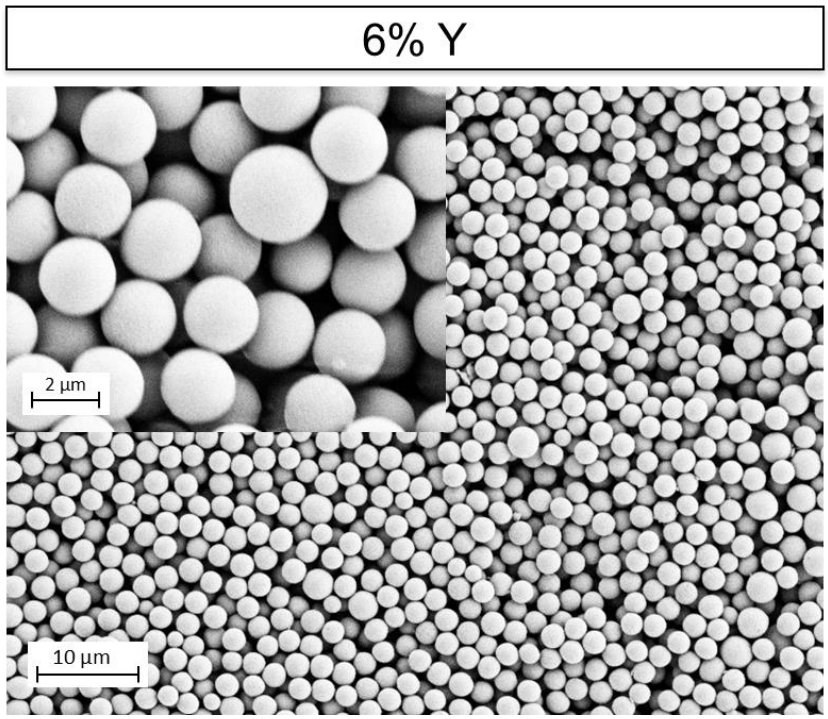

Figure S 14. Film F6 assembled from particle sample YPG6 after heating at 700 °C for 3h.

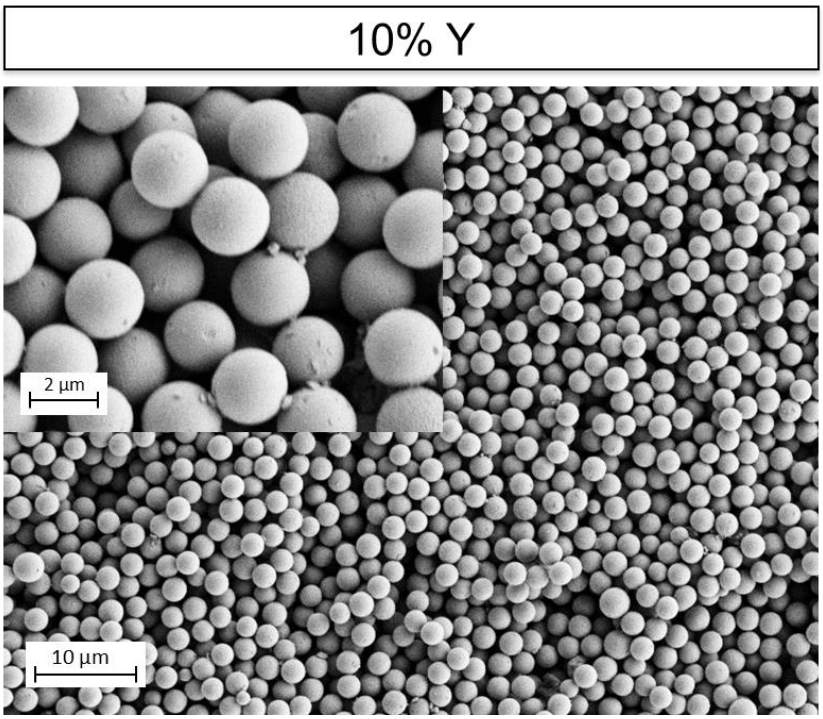

Figure S 15. Film F10 assembled from particle sample YPG10 after heating at 700 °C for 3h.

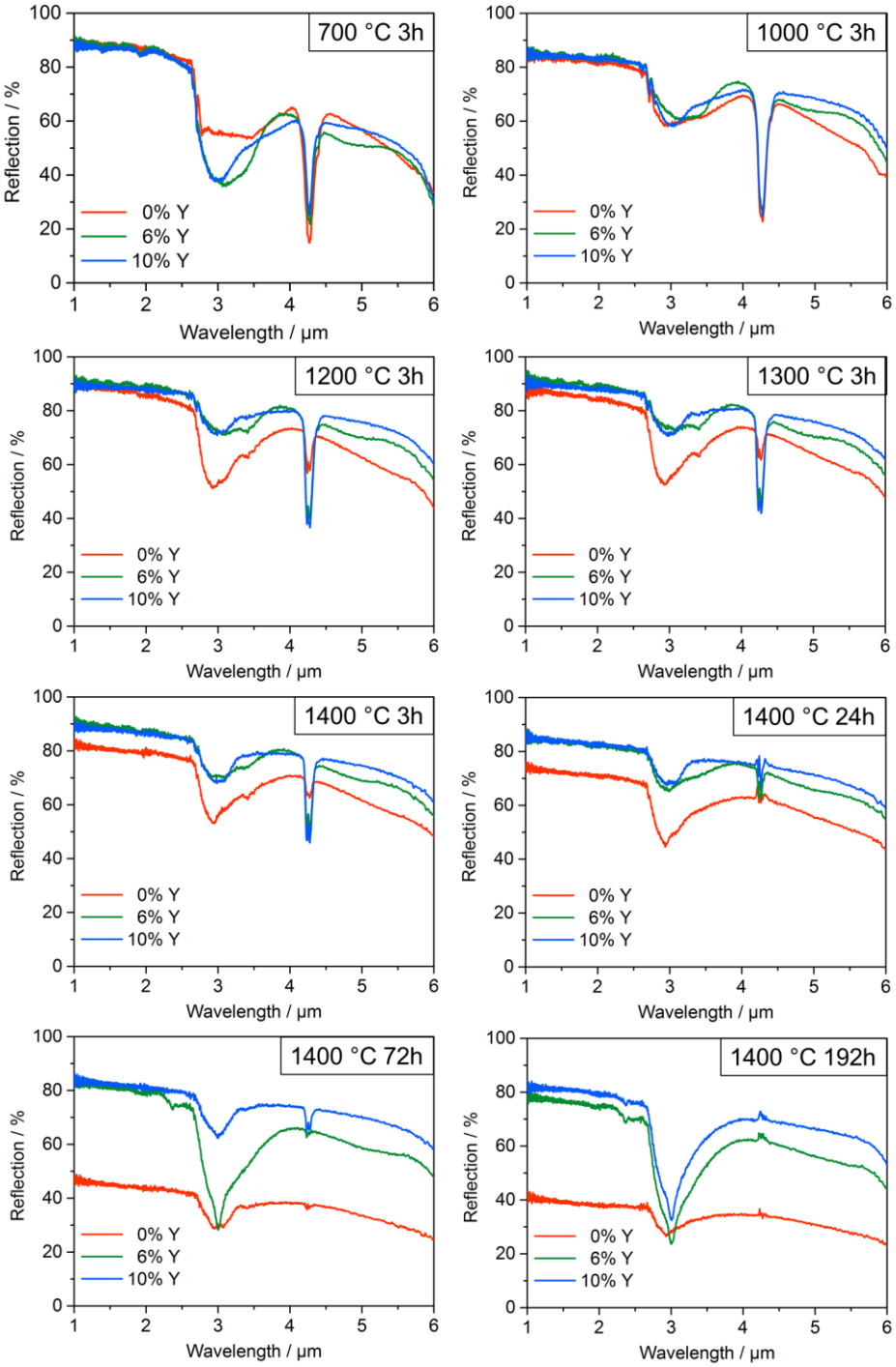

Figure S 16. Hemispherical diffuse reflection for samples F0, F6 and F10 after each heating cycle.

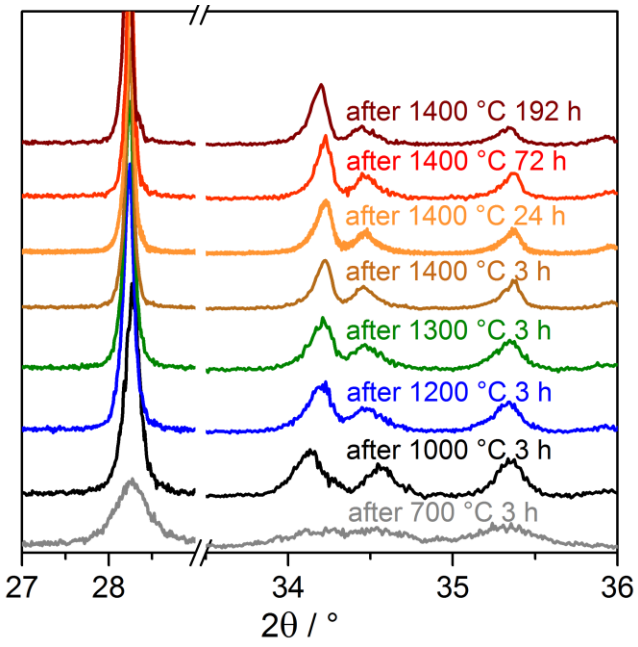

Figure S 17. X-ray diffractograms of film sample F0 after each heating cycle.

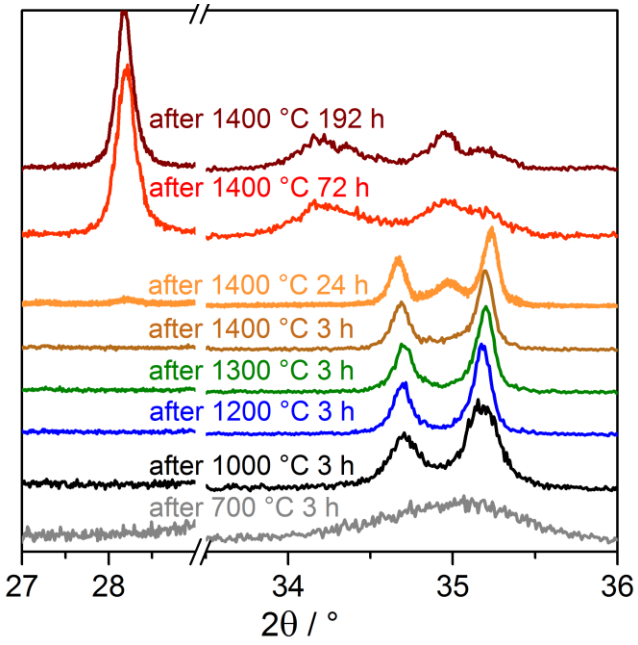

Figure S 18. X-ray diffractograms of film sample F6 after each heating cycle.

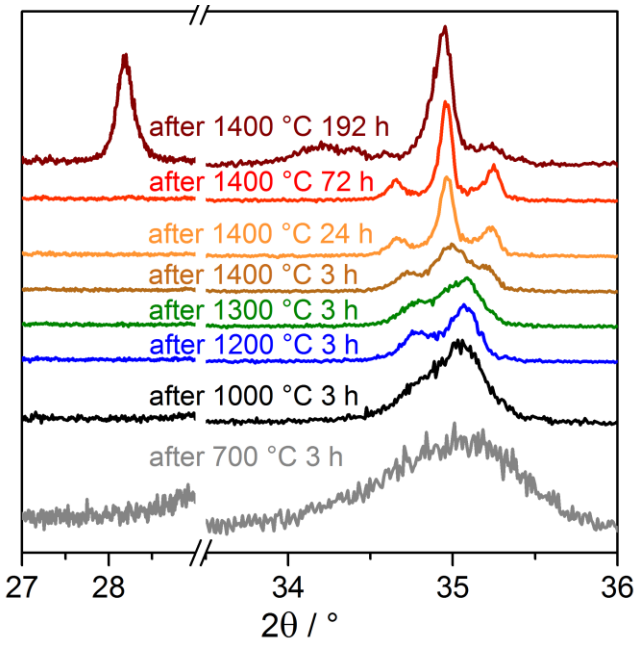

Figure S 19. X-ray diffractograms of film sample F10 after each heating cycle.

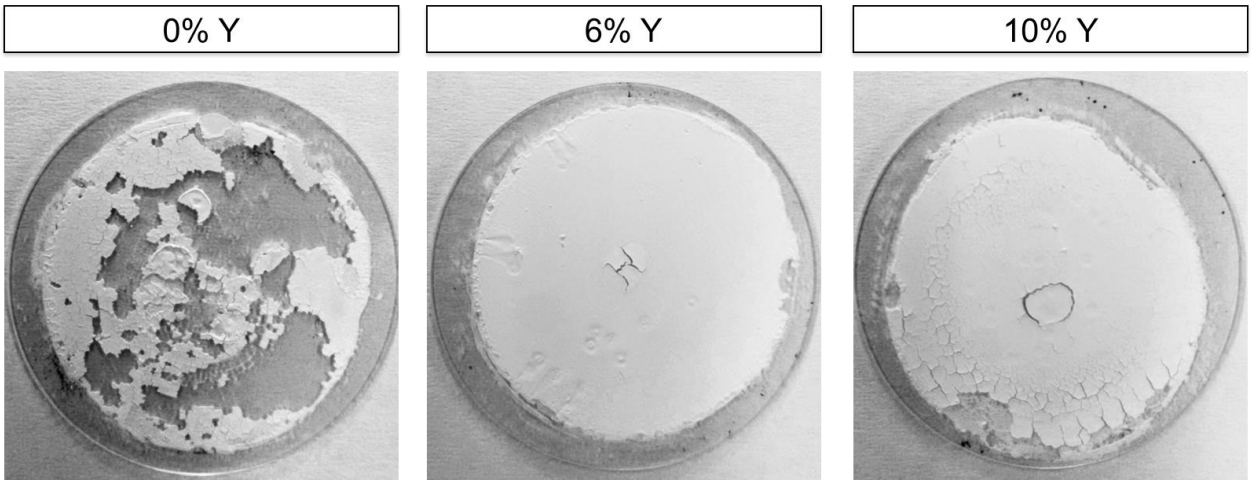

Figure S 20. Photographs of film samples F0, F6 and F10 after heating at 1400 °C for a total of 72 h.